 CMC, vol.54, no.3, pp.287-306, 2018

Effect of Different Shapes of Conformal Cooling Channel on the Parameters of Injection Molding

Mahesh S. Shinde[1, *] and Kishor M. Ashtankar[1]

Abstract: Cooling system improvement is important in injection molding to get better quality and productivity. The aim of this paper was to compare the different shapes of the conformal cooling channels (CCC) with constant surface area and CCC with constant volume in injection molding using Mold-flow Insight 2016 software. Also the CCC results were compared with conventional cooling channels. Four different shapes of the CCC such as circular, elliptical, rectangular and semi-circular were proposed. The locations of the cooling channels were also kept constant. The results in terms of cooling time, cycle time reduction and improvement in quality of the product shows that no significant effect of CCC's shapes when surface area of CCC kept constant. On the other hand, the rectangular CCC shows better result as compared to other shapes of CCC when volume of CCC were kept constant.

Keywords: Injection mold, conformal cooling channels, cooling simulation, rapid tooling.

1 Introduction

Cooling channel in shape of the part is called as conformal cooling channel (CCC). Fig. 1 shows the straight-drilled (conventional) and conformal (non-conventional) cooling channels. The main purpose of CCC design is to obtained uniform cooling and reduction of cooling time. CCC has been proven more efficient as compared to the conventional cooling channels in terms of a rate of production and accuracy of molded parts. [Dimla, Camilotto and Miani (2005); Saifullah and Masood (2007)].

Rapid tooling (RT) is the advanced manufacturing technique which is widely used for the CCC fabrication. These RT methods are classified into two types, namely as direct and indirect RT. In the direct RT, molds are directly fabricated using Rapid Prototyping (RP). In the indirect RT method a RP pattern is converted into a mold using secondary manufacturing techniques [Nagahanumaiah and Ravi (2009)]. Rapid prototyping assisted CCC in the mold reduces cooling time and cycle time, provide uniform thermal distribution, and improve part deflection [Shinde and Ashtankar (2017)].

[1] Department of Mechanical Engineering, Visvesvaraya National Institute of Technology, Nagpur-440010, India.

[*] Corresponding author: Mahesh S. Shinde. Email: maheshsshinde@ymail.com.

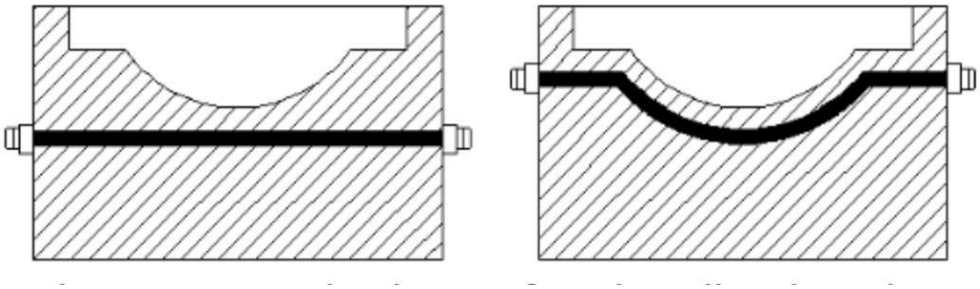

Figure 1: Conventional & conformal cooling channels [Altaf, Raghavan and Rani (2011)]

Au et al. [Au and Yu (2007)] recommended a scaffolding architecture for CCC design. The comparison of mold cavity with and without scaffolding structure was studied using simulation technique. Mold flow analysis of the porous scaffolding structure was done by Moldflow plastics insight 3.1. The scaffold cooling system provided better cooling in mold cavity. They found greater surface area for the cooling in scaffolding cooling system as compared to the conventional straight-drilled and copper duct bending cooling systems, resulting in uniform distribution of heat.

The CCC using an array of baffles was investigated by researcher in the plastic injection molds for a radiator grill with ABS 750 material. The performance of cooling channels was evaluated and compared with the results of an array of baffles with the straight cooling channels using Moldflow software. From the analysis, the temperature variation in cooling channel with an array of baffles was improved by 49%, which is more uniform as compared to the straight cooling channels [Park and Dang (2010)].

Au et al. [Au and Yu (2011)] proposed an alternative design method for a CCC with multi-connected porous characteristics based on the duality principle. The proposed method provides a more uniform cooling performance than the existing CCC design.

Wang et al. [Wang, Yu, Wang et al. (2011)] investigated a geometric modeling Vornoi Diagram (VD) based algorithm to design the cooling circuit approaching CCC. As compared to previous methods, this approach offered the advantages of automatic generation of CCC as per the shape of products. The results showed that this method effectively reduced the cooling time and controlled the uniformity of temperature and volumetric shrinkage. The limitation of this algorithm was that, it requires iterative optimization procedure to adjust the cooling channels by correcting the cycle time.

Au et al. [Au and Yu (2014)] were presented a novel adjustment method for cooling distance modification between the CCC and its mold cavity (or core) surface along the cooling channel. The method can balance the gradual increase of the coolant temperature from the coolant inlet to the coolant outlet. More heat can be transferred from the mold surface near the coolant outlet to the variable distance conformal cooling channel (VDCCC).

Wang et al. [Wang, Yu, Wang et al. (2015)] introduced a new approach for generation of spiral CCC and compared with VD-based CCC. They found less cooling time with spiral CCC than VD based CCC.

Brooks et al. [Brooks and Brigden (2016)] introduced the concept of CCC layers which provides higher heat transfer rates and less variation in tooling temperatures. The cooling layers are filled with self-supporting repeatable unit cells that form a lattice throughout the cooling layers. The lattice helps to improve convective heat transfer.

Hearunyakij et al. [Hearunyakij, Masood and Sbarski (2014)] has proved that fin type of CCC helps to improve efficiency of cooling. In another study author compared results of square section conformal cooling channel (SSCCC) with conventional straight cooling channels (CSCC) in an injection-molding process by using Mold-flow plastic insight software. The simulated results confirmed that using PP and ABS as the plastic materials with normal water 25°C, as a coolant was reduced the cooling time by 35% with the SSCCC as compared to the CSCC. The cycle time was also reduced by 20% by using the SSCCC than CSCC [Safullah, Masood and Sbarski (2009)].

Straight drilled CC compared with MGCCC by using Autodesk Moldflow Insight (AMI) 2016 software. A case study of Enclosure part investigated for cycle time reduction and quality improvement. The simulation results showed 32.1% reduction of cooling time and 9.86% reduction of warpage in case of MGCCC as compared to conventional cooling [Shinde and Ashtankar (2017); Panthi and Saxena (2012)]

In another study researchers compared the results of profiled cross sectional CCC with circular cross sectional CCC. Both channels designed with 78.5 mm^2 cross-section areas and normal water 25°C was used as a coolant. The thermal distribution in both the CCC was simulated by using ANSYS. Result showed 14.6% increase of heat flow with profile cross sectional CCC [Altaf, Raghavan and Rani (2011)]. To determine the optimal process parameters CAE simulation is widely used and is recognised as one of the powerful tools based on Finite Element method (FEM) [Wei, Chen, Chen et al. (2016); Panthi and Saxena (2012); Shiah, Lee and Wang (2013); Essam, Mhamed and Thamar (2015); Ma, Sato and Takada (2015)].

In this paper, the effect of the cooling channels position and their form on the solidification and temperature distribution are studied during the cooling of Zytel 70G33L NC010 thermoplastic material by injection molding. Study focuses on comparison of different shapes of CCC by keeping constant surface area and constant volume of CCC. Also these CCCs were compared with conventional cooling channels. Four forms of the CCC shape such as circular, elliptical, rectangular and semi-circular with constant location were proposed.

2 Material and methods

2.1 Numerical model

In this study, three-dimensional, cyclic, transient heat conduction problem with convective boundary conditions on the cooling channel and mold base surfaces for the cooling stage of plastic injection molding is involved. The heat transfer equation is based on a three-dimensional Poisson Eq. (1),

$$\rho C_p \frac{\partial T}{\partial t} = k\left(\frac{\partial^2 T}{\partial x^2} + \frac{\partial^2 T}{\partial y^2} + \frac{\partial^2 T}{\partial z^2}\right) \quad (1)$$

Where T is the temperature, t is the time, ρ is the density, Cp is the specific heat, k is the thermal conductivity and x, y, z are the Cartesian coordinates.

Eq. (1) holds for both mold base and plastic part with modification on thermal properties.

The initial part temperature distribution is received from the analysis results at the end of filling and packing stages. The initial mold temperature is assumed to be equal to the coolant temperature.

For this research, the effect of thermal radiation is disregarded. The conditions defined over the boundary surfaces and interfaces of the mold are specified by Eq. (2),

$$-k_m \frac{\partial T}{\partial n} = h(T_{ini} - T_0) \tag{2}$$

Where km is the thermal conductivity of mold and n is the normal direction of mold boundary.

Heat from the molten plastic part is released by the coolant flowing in cooling channel as well as the ambient air surrounding the exterior surfaces of the mold base through a heat convection mechanism.

On the exterior surfaces of the mold base

$h = h_{air}, \quad T_0 = T_{air}$

On the cooling channel surfaces

$h = h_c, \quad T_0 = T_c$

Where hair and hc are heat transfer coefficients of air and coolant

2.2 Part modeling

The part chosen for this study is an injection moulded plastic part made of Zytel 70G33L NC010 thermoplastic. Actual mould for this part is of multi cavities mould, but only single cavity type has been considered for this investigation. Fig. 2 shows the CAD model of the plastic part, wall thickness of 1.5 mm with feed system.

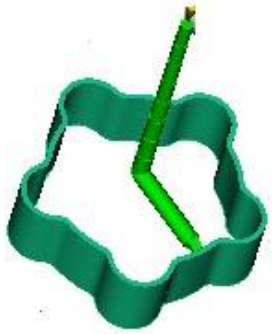

Figure 2: Part model with gating system

2.3 Mold-flow analysis for plastic injection molding

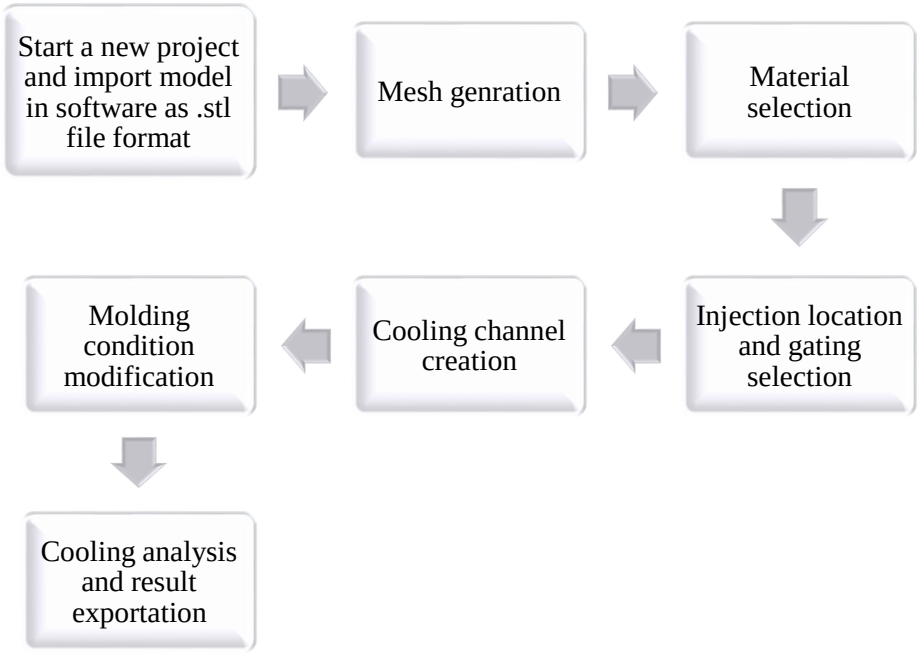

Figure 3: Steps of plastic part analysis in Mold-flow Insight software

In this study, simulation was performed in the injection molding software-Mold-flow Insight 2016. Steps followed for analysis through Mold-flow Insight 2016 software are given in the Fig. 3. For the cooling analysis a uniform initial temperature (i.e. the melt temperature) was assumed for the melt of polymer.

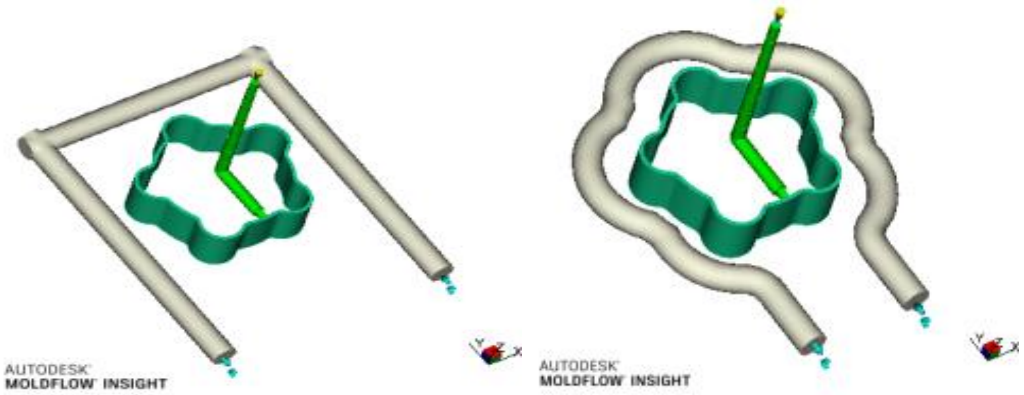

(a) (b)

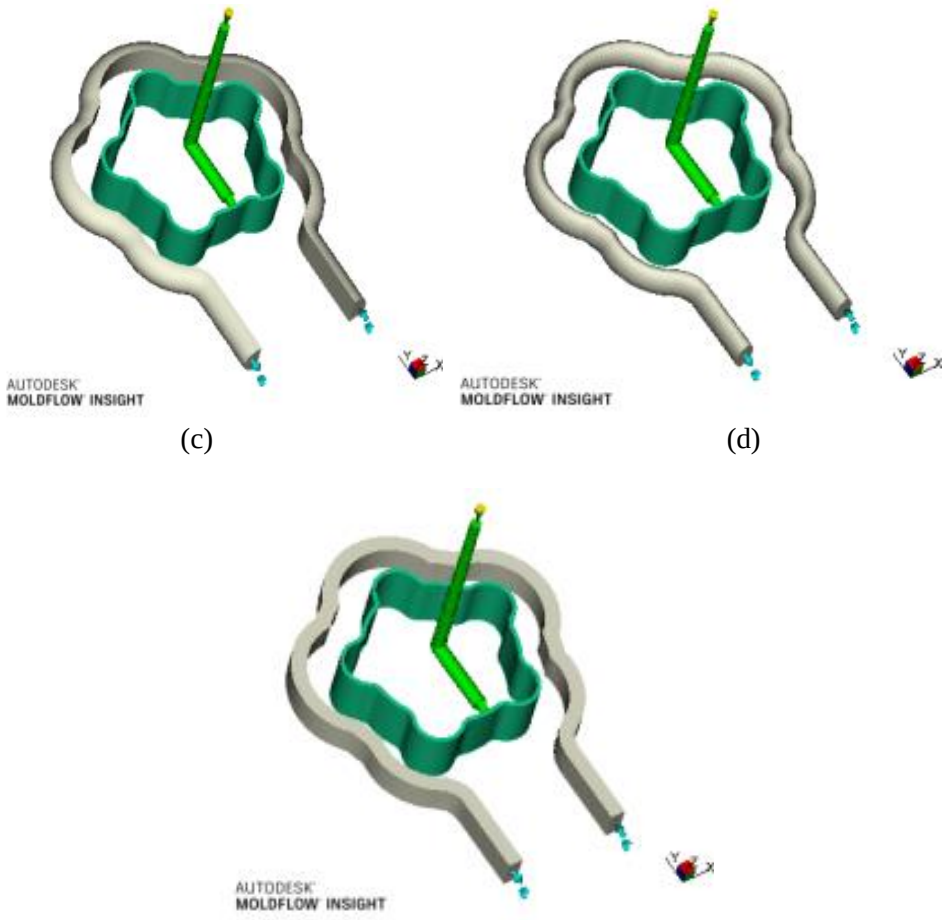

(c) (d)

(e)

Figure 4: Different types of cooling channels: (a) conventional; (b) circular CCC; (c) semicircular CCC; (d) elliptical CCC; (e) rectangular CCC

In first step preparation of 3D CAD model of plastic part and injection mold systems including different types of cooling channels were created in Solid-works (Fig. 4). After that meshing of all components were performed in Mold-flow Insight 2016. In order to estimate cooling time of part model, auto set cooling time command in Mold-flow Insight 2016 was applied for cool (FEM) analysis. The following injection mold conditions were set for analysis.

- Part material=Zytel 70G33LNC010
- Mold material=P20 steel
- Melt temperature=300 [°C]
- Filling time=1 [s]
- Packing time=5 [s]
- Packing pressure=40 [MPa]

- Initial mold temperature=70°C
- Initial coolant temperature=70°C
- Coolant velocity=15 lit/min
- Coolant type=water

The similar parameters were used in all cases for analysis.

3 Design of cooling channel

3.1 CCC design with constant surface area

In this research, the study and the development of conformal cooling system focused on comparison of different shapes of cooling channels. Part model, injection condition and cooling flow lines kept similar for each case for comparison of cooling efficiency. The distance between cavity surface and tangent of cooling channel has taken 10 mm constant for each case. According to the part thickness, the diameter (D) of cooling channel was considered 10 mm for circular cooling channel. Based on dimensions of circular CCC remaining shapes dimensions were calculated by keeping surface area constant. Surface area is the parameters of length and perimeter of CCC. Length of CCC was same in each case. So the perimeters of all the shapes were constant.

$$\boldsymbol{A = L \times P} \tag{3}$$

Where A Surface area of cooling channel P is perimeter and l is length of cooling channel.

$$P_c = 2\pi R_c \tag{4}$$

Where Pc is perimeter of circle and Rc is radius of circle.

$$P_s = (2 + \pi)R_s \tag{5}$$

Where Ps is perimeter of semi-circle and Rs is radius of semi-circle.

$$P_r = 2(b + d) \tag{6}$$

Where Pr is perimeter of rectangle, b is the width and d is height of rectangle where d=2b.

$$\mathrm{P_e} = 2\pi \sqrt{\frac{(\mathrm{a^2 + b^2})}{2}} \tag{7}$$

Where Pe is perimeter of ellipse, a is the major and b is minor radius of ellipse where a=2b.

Dimensions were calculated from equating Eqs. (4-7) for circle Rc=5 mm, for semicircle Rs=6.10 mm, for rectangle d=10.46 mm, b=5.23 mm and for ellipse a=6.32 mm, b=3.16 mm. With these dimensions modeling of different shapes of CCC was done.

3.2 Results for constant surface area of CCC

Results have investigated through Mold-flow Insight 2016 and compared the cooling performances such as the part temperature, cooling circuit temperature, mold interface temperature, and cooling time between the conventional design and the different shapes of CCC for constant surface area.

The part temperature obtained for conventional cooling channel was 168.9°C and for circular, elliptical, semi-circular, and rectangular shape CCC was 166.8, 166.9, 166.9, 166.9°C respectively (Fig. 5). The cooling circuit temperature achieved for conventional

cooling channel was 70.7°C and for the circular, elliptical, semi-circular, and rectangular shape CCC was 71.44, 71.44, 71.45, 71.43°C respectively (Fig. 6). The mold interface temperature for conventional cooling channel was found 83.87°C and for the circular, elliptical, semi-circular, rectangular shape CCC was 81.84, 81.81, 81.83, 81.84°C respectively (Fig. 7). The cooling time for the conventional cooling channel was obtained as 3.125 sec and for the circular, elliptical, semi-circular, rectangular shape CCC was 3.092, 3.093, 3.092, 3.092 sec respectively (Fig. 8).

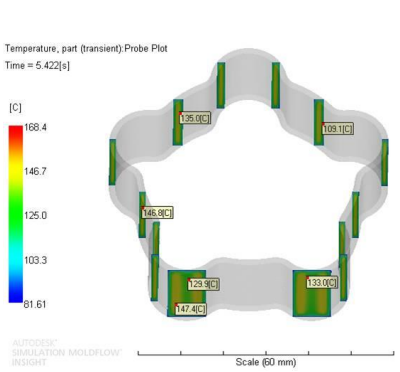

(a)

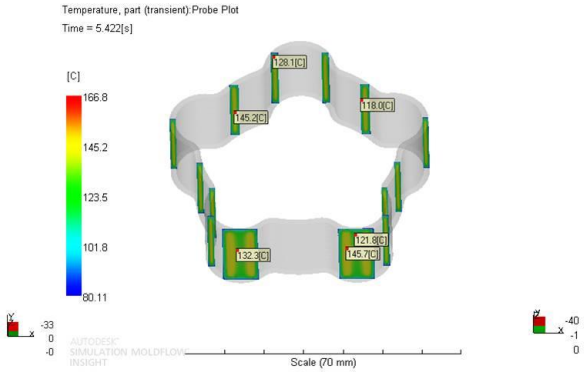

(b)

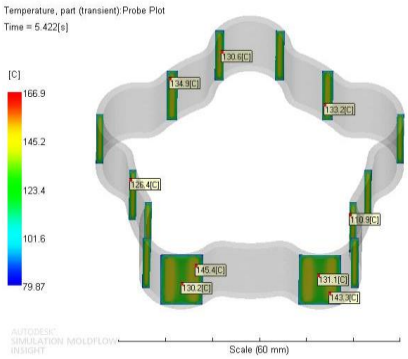

(c)

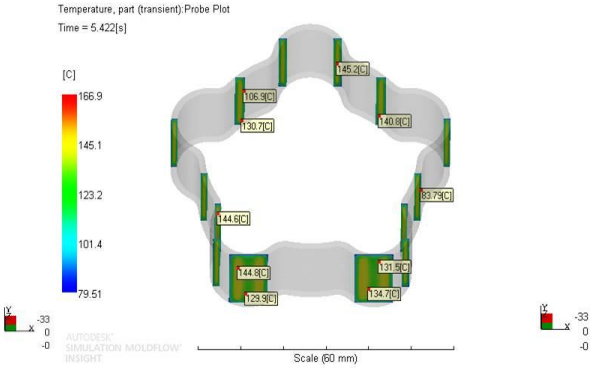

(d)

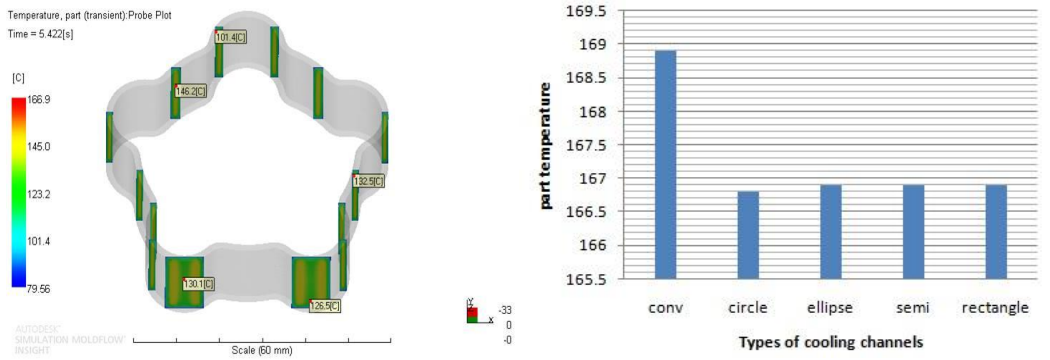

(e) (f)

Figure 5: Results and comparisons of different types of cooling with part temperature: (a) conventional; (b) circular CCC; (c) elliptical CCC; (d) semicircular CCC; (e) rectangular CCC; (f) comparative bar chart

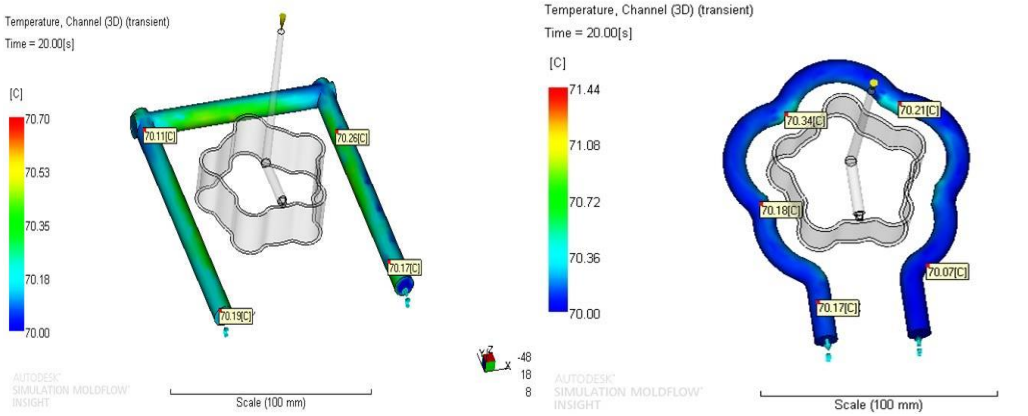

(a) (b)

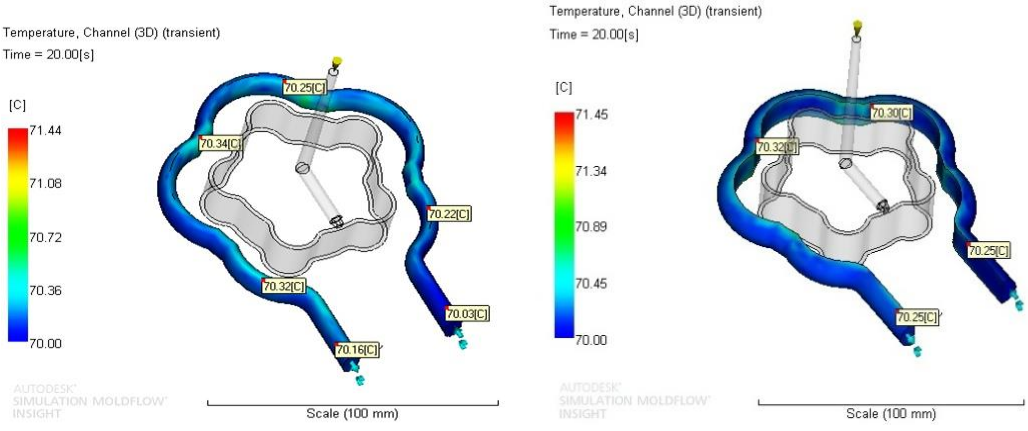

(c) (d)

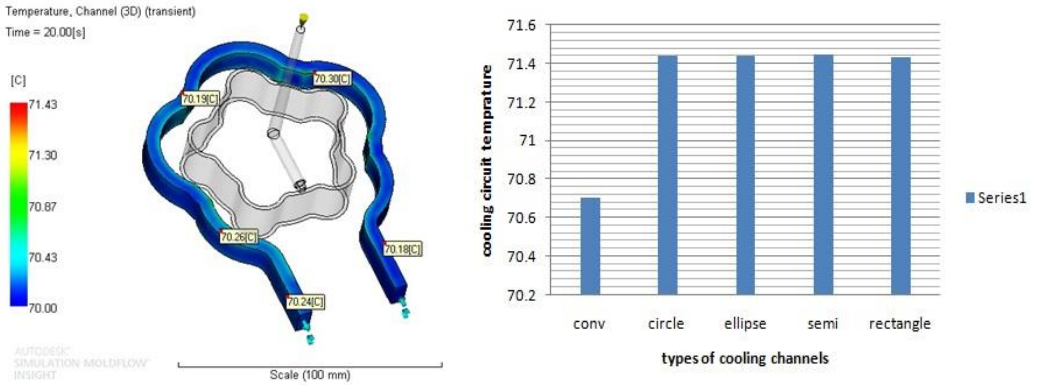

(e) (f)

Figure 6: Results and comparisons of different types of cooling with cooling circuit temperature: (a) conventional; (b) circular CCC; (c) elliptical CCC; (d) semicircular CCC; (e) rectangular CCC; (f) comparative bar chart

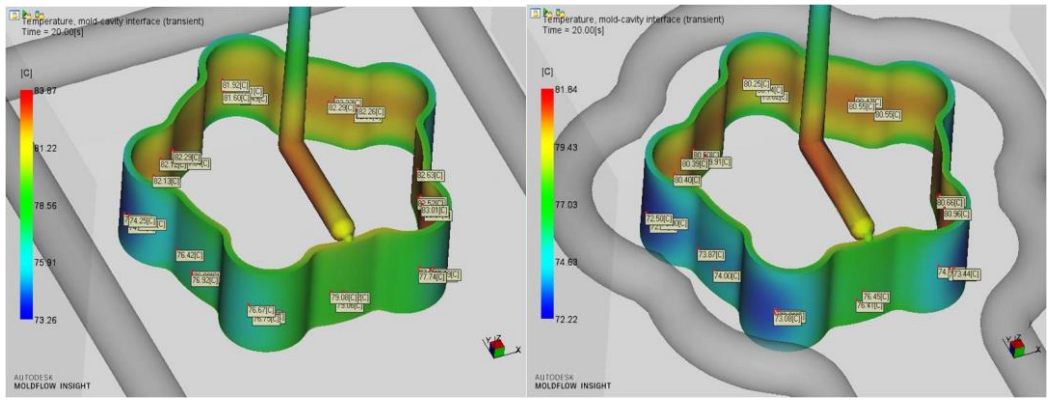

(a) (b)

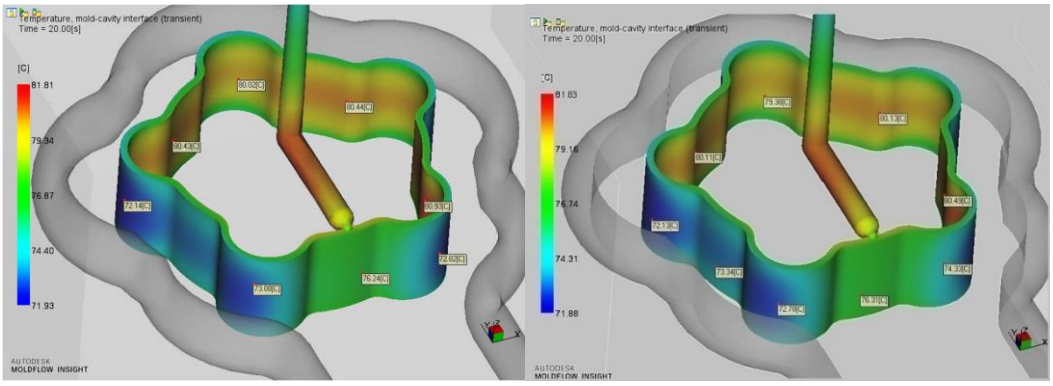

(c) (d)

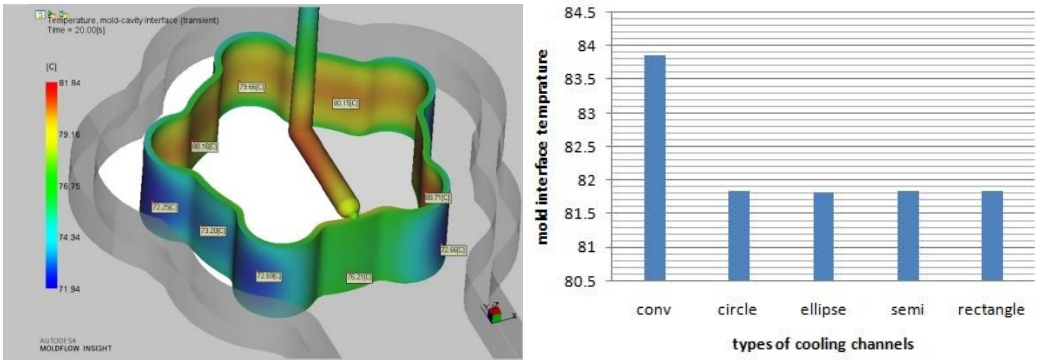

(e) (f)

Figure 7: Results and comparisons of different types of cooling with mold interface temperature: (a) conventional; (b) circular CCC; (c) elliptical CCC; (d) semicircular CCC; (e) rectangular CCC; (f) comparative bar chart

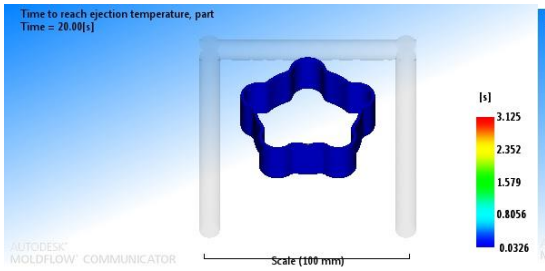

(a)

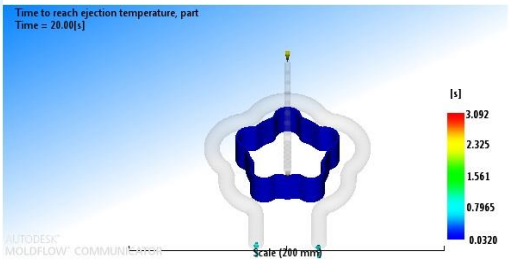

(b)

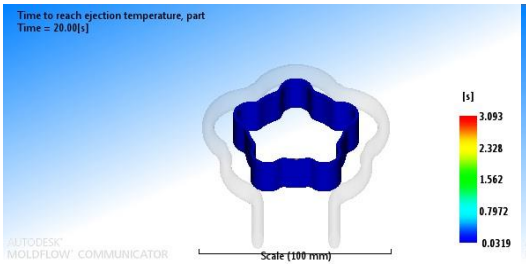

(c)

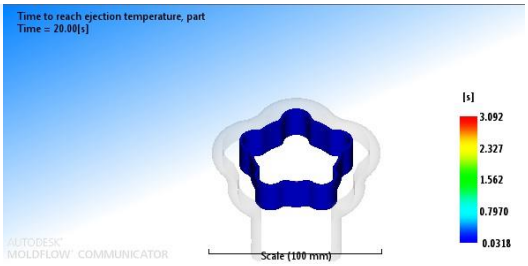

(d)

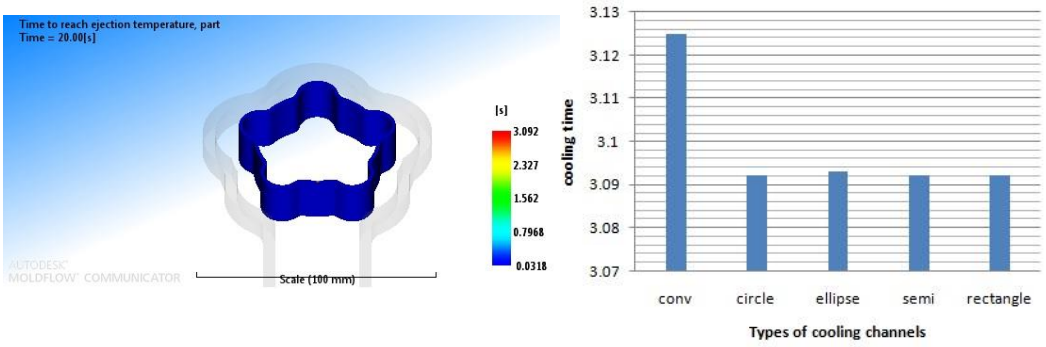

(e) (f)

Figure 8: Results and comparisons of different types of cooling with cooling time: (a) conventional; (b) circular CCC; (c) elliptical CCC; (d) semicircular CCC; (e) rectangular CCC; (f) comparative bar chart

The almost similar results in terms of part temperature, cooling circuit temperature, mold interface temperature, and cooling time were obtained for different shapes of CCC. However, as compare to conventional cooling channels CCC results were showing reduction in part temperature; improvement in cooling circuit temperature; reduction in the mold interface temperature; and reduction in the cooling time.

3.3 CCC design with constant volume

According to part thickness, the diameter (D) of cooling channel was considered 10 mm for circular CCC Distance between cavity surface and tangent of cooling channel was 10 mm, by keeping volume of the CCC constant other shapes of CCC dimensions were calculated. In each case the length of cooling channel was equal.

$$V = A_{cs} \times L \tag{8}$$

Where V is the volume of the cooling channel, Acs is the cross-section area of cooling channel and L is the length of cooling channel.

$$A_c = \pi {R_c}^2 \tag{9}$$

Where Ac is cross section area of circle and Rc is radius of circle.

$$A_s = \frac{\pi}{2} {R_s}^2 \tag{10}$$

Where As is cross section area of semi-circle and Rs is radius of semi-circle.

$$A_r = b \times d \tag{11}$$

Where Ar is cross section area of rectangle, b is the width and d is height of rectangle where d=2b.

$$A_e = \pi \times a \times b \tag{12}$$

Where A_e is cross section area of ellipse, a is the major and b is minor radius of ellipse where a=2b.

The The diameter (D) of cooling channel was considered 10 mm for circular cooling channel. Based on dimensions of circular CCC remaining shapes dimensions were

calculated by keeping volume constant. As volume is parameter of cross section area and length and length of the cooling channel was same. Cross section area of different shapes kept constant and dimensions calculated from equating Eqs. (9-12) for circle Rc=5 mm considered from that for Semicircle Rs=7.07 mm, for Rectangle d=12.52 mm, b=6.26 mm and for Ellipse a=7.07 mm, b=3.535 mm. With these dimensions, modeling of different shapes of CCC was done. Same analysis was done with same parameters as previous analysis in constant surface area case and results shown in Figs. 9-12 for different shapes of CCC with constant volume.

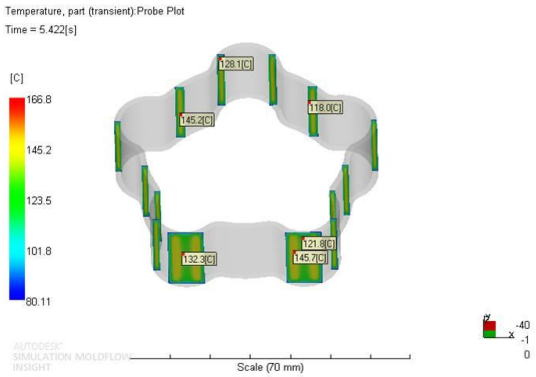

(a)

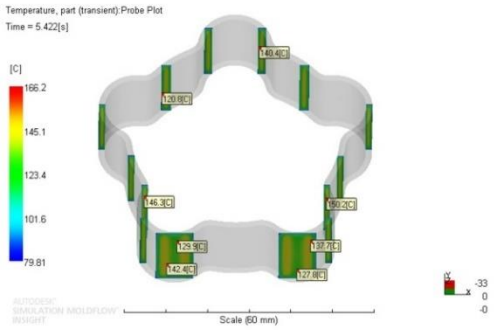

(b)

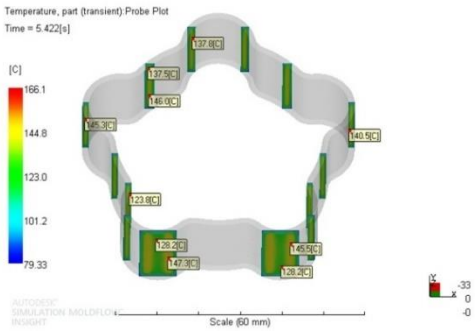

(c)

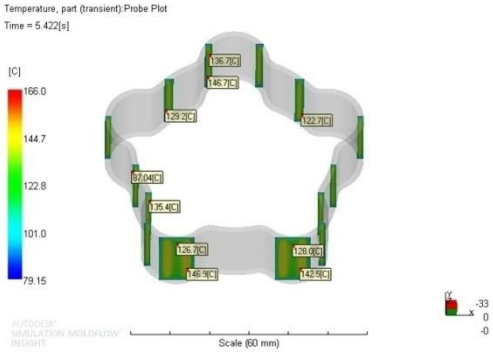

(d)

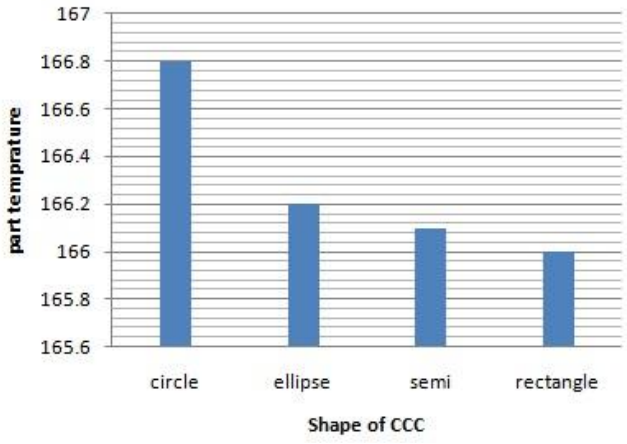

(e)

Figure 9: Results and comparisons of different shapes of CCC with part temperature: (a) circular CCC; (b) elliptical CCC; (c) semicircular CCC; (d) rectangular CCC; (e) comparative bar chart

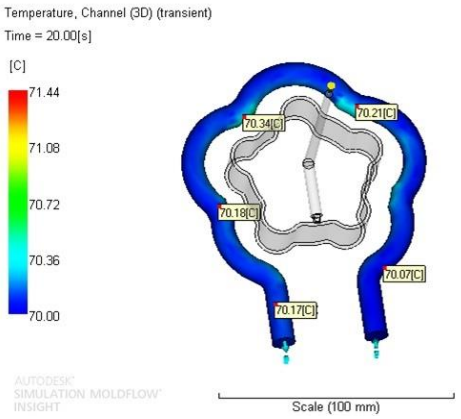

(a)

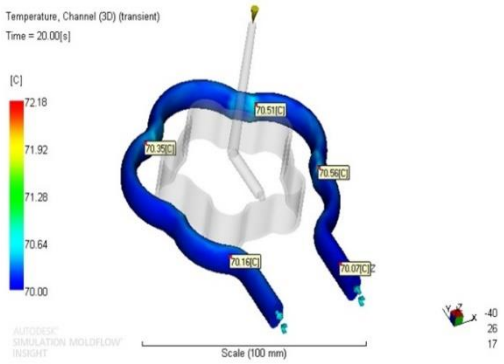

(b)

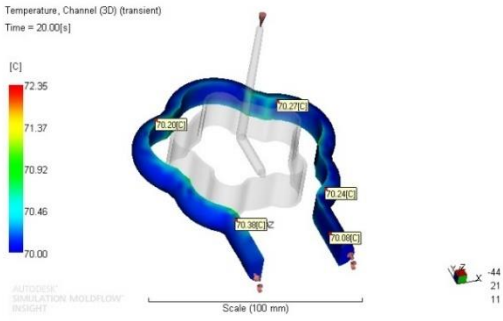

(c)

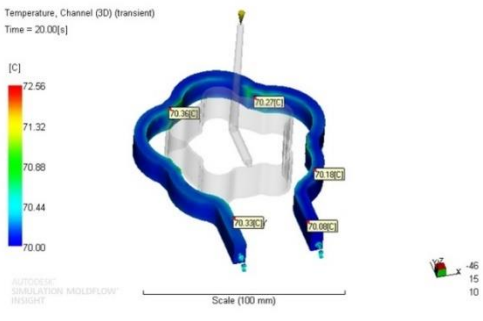

(d)

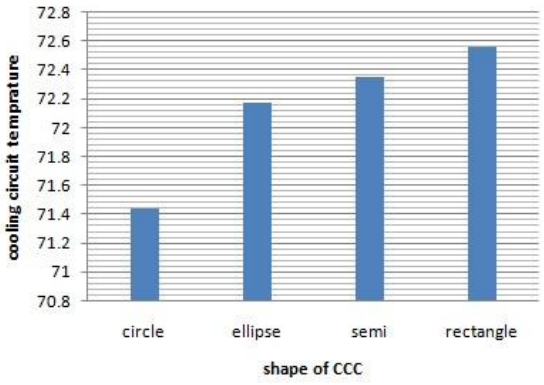

(e)

Figure 10: Results and comparisons of different shapes of CCC with cooling circuit temperature: (a) circular CCC; (b) elliptical CCC; (c) semicircular CCC; (d) rectangular CCC; (e) comparative bar chart

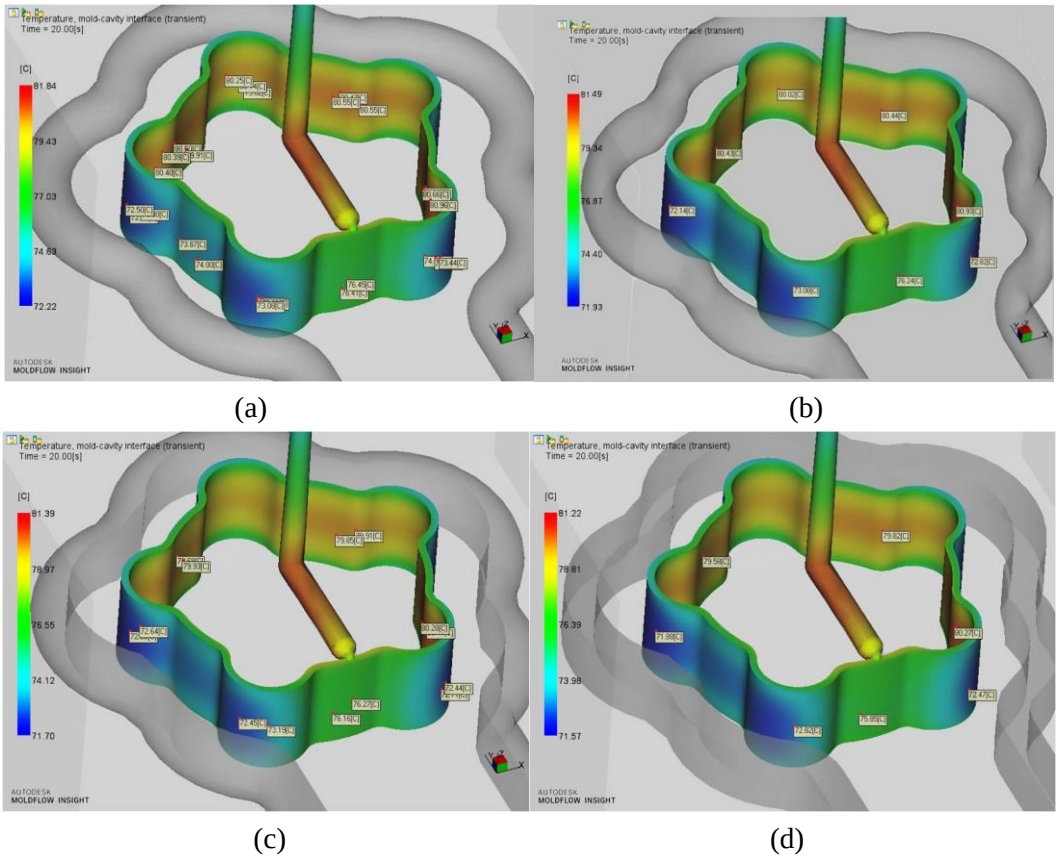

(a) (b)

(c) (d)

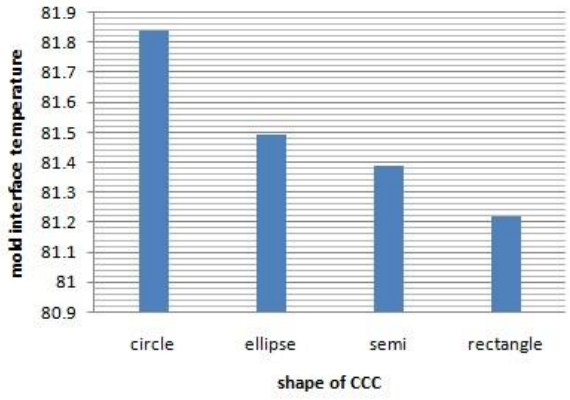

(e)

Figure 11: Results and comparisons of different shapes of CCC with mold interface temperature: (a) circular CCC; (b) elliptical CCC; (c) semicircular CCC; (d) rectangular CCC; (e) comparative bar chart

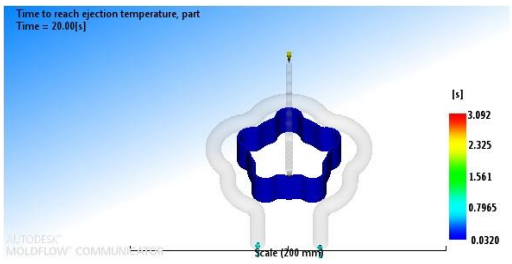

(a)

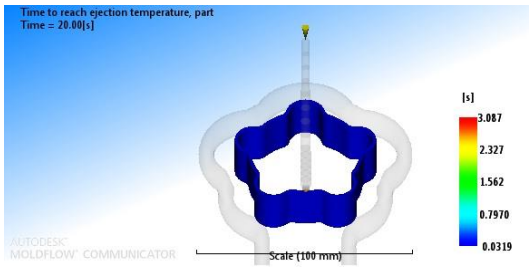

(b)

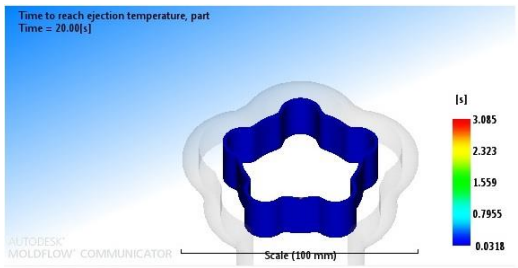

(c)

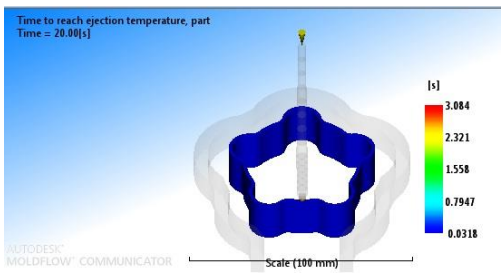

(d)

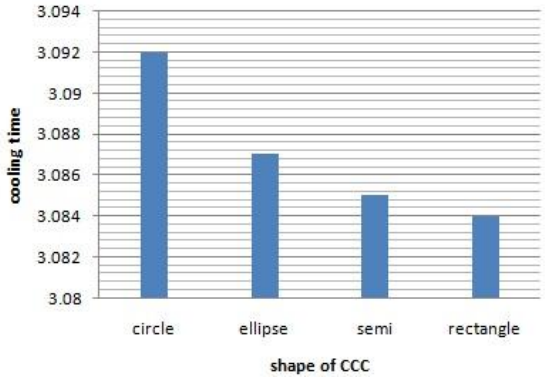

(e)

Figure 12: Results and comparisons of different shapes of CCC with cooling time: (a) circular CCC; (b) elliptical CCC; (c) semicircular CCC; (d) rectangular CCC; (e) comparative bar chart

3.4 Result for constant volume of CCC

As in first case (constant surface area of CCC) overall results of different shapes seems to be similar. Again for the next case (volume of CCC constant) results have investigated using Mold-flow Insight 2016 and compared the cooling performances in terms of the part temperature, cooling circuit temperature, mold interface temperature, and cooling time between the different shapes of CCC.

For the circular, elliptical, semi-circular, and rectangular shape CCC the part temperature was obtained as 166.8, 166.2, 166.1, 166.0°C respectively (Fig. 9), the cooling circuit temperature was 71.44, 72.18, 72.35, 72.56°C respectively (Fig. 10), the mold interface temperature was 81.84, 81.49, 81.39, 81.22°C respectively (Fig. 11), and the cooling time achieved was 3.092, 3.087, 3.085, 3.084 sec respectively (Fig. 12).

It was showing that results of part temperature, cooling circuit temperature, mold interface temperature, and cooling time were changing with different shapes of CCC. The rectangular CCC obtained better results as compare to remaining shape CCC. For the rectangular CCC the lowest part temperature was obtained i.e. 166.0°C, the highest cooling circuit temperature i.e. 72.56°C, the lowest mold interface temperature i.e. 81.22°C, and the shortest cooling time 3.084 sec.

4 Discussion

In this analysis perimeter of CCC was 31.41 mm for all shapes of CCC from that dimensions of different shapes of CCC were calculated. It was showing quite similar results for different shapes of CCC because surface area of each CCC was constant.

In this analysis cross section area of CCC was 78.53 mm^2 for all shapes of CCC from that dimensions of different shapes of CCC calculated and results showing rectangular CCC have better cooling results because surface area of rectangular cooling was more as

compared to all other shapes. Total comparisons of results with different parameters are shown in Tab. 1.

Table 1: Results of different cooling with different parameters

Parameters	Types of cooling channels								
	Regular	Constant surface area				Constant volume of the coolant			
	Straight drilled	circle CCC	Ellipse CCC	Semi circle CCC	Rectangle CCC	circle CCC	Ellipse CCC	Semi circle CCC	Rectangle CCC
Part temperature (°C)	168.9	166.8	166.9	166.9	166.9	166.8	166.2	166.1	166.0
Cooling circuit temperature (°C)	70.70	71.44	71.44	71.45	71.43	71.44	72.18	72.35	72.56
Mold interface temperature (°C)	83.87	81.84	81.81	81.83	81.84	81.84	81.49	81.39	81.22
Cooling time (sec)	3.125	3.092	3.093	3.092	3.092	3.092	3.087	3.085	3.084

5 Conclusion

According to the results obtained in the analyses conducted in this study, the following conclusions can be drawn

- Conformal cooling gives better results as compared to conventional cooling
- Reduction in cooling time in case of CCC as compared to conventional cooling
- Surface area of CCC is the important parameter for cooling analysis irrespective of shape of CCC
- In case of constant volume of CCC, rectangular CCC gives better results as it is having more surface area as compared to the shapes of CCC

Reference

Altaf, K.; Raghavan, V. R.; Rani, A. M. A. (2011): Comparative Thermal Analysis of Circular and Profiled Cooling Channels for Injection Mold Tools. *Journal of Applied Sciences*, vol. 11, pp. 2068-2071.

Au, K. M.; Yu, K. M. (2007): A scaffolding architecture for conformal cooling design in rapid plastic injection molding. *International Journal of Advanced Manufacturing Technology*, vol. 34, no. 5, pp. 496-515.

Au, K. M.; Yu, K. M. (2011): Modeling of multi-connected porous passageway for mould cooling. *Computer Aided Design*, vol. 43, no. 8, pp. 989-1000.

Au, K. M.; Yu, K. M. (2014): Variable radius conformal cooling channel for rapid tool. *Journal of Manufacturing Science and Engineering*, vol. 136, no. 4, pp. 1-9.

Brooks, H.; Brigden, K. (2016): Design of conformal cooling layers with self-supporting lattices for additively manufactured tooling. *Additive Manufacturing*, vol. 11, pp. 16-22.

Dimla, D. E.; Camilotto, M.; Miani, F. (2005): Design and optimisation of conformal cooling channels in injection molding tools. *Journal of Materials Processing Technology*, vol. 164-165, pp. 1294-1300.

Essam, A. B.; Mhamed, S.; Thamar, A. B. (2015): SPH and FEM investigation of hydrodynamic impact problems. *Computers, Materials & Continua*, vol. 46, no. 1, pp. 57-78.

Hearunyakij, M.; Sontikaew, S.; Sriprapai, D. (2014): Improvement in the cooling performance of conformal mold cooling by using fin concept. *International Journal of Mining, Metallurgy & Mechanical Engineering*, vol. 2, no. 2, pp. 41-46.

Ma, N.; Sato, K.; Takada, K. (2015): Analysis of local fracture strain and damage limit of advanced high strength steels using measured displacement fields and FEM. *Computers, Materials & Continua*, vol. 46, no. 3, pp. 195-219.

Nagahanumaiah; Ravi, B. (2009): Effects of injection molding parameters on shrinkage and weight of plastic part produced by DMLS mold. *Rapid Prototyping Journal*, vol. 15, no. 3, pp. 179-186.

Panthi, S. K.; Saxena, S. (2012): Prediction of crack location in deep drawing processes using finite element simulation. *Computers, Materials & Continua*, vol. 32, no. 1, pp. 15-27.

Park, H. S.; Dang, X. P. (2010): Structural optimization based on CAD-CAE integration and metamodeling techniques. *Computer-Aided Design*, vol. 42, no. 10, pp. 889-902.

Safullah, A. B. M.; Masood, S. H.; Sbarski, I. (2009): Cycle time optimization and part quality improvement using novel cooling channels in plastic injection molding. *Society of Plastics Engineers*.

Saifullah, A. B. M.; Masood, S. H. (2007): Cycle time reduction in injection molding with conformal cooling channels. *Proceedings of the International Conference on Mechanical Engineering*, Dhaka, Bangladesh.

Shiah, Y. C.; Lee, Y. M.; Wang, C. C. (2013): BEM analysis of 3D heat conduction in 3D thin anisotropic media. *Computers, Materials & Continua*, vol. 33, no. 3, pp. 229-255.

Shinde, M. S.; Ashtankar, K. M. (2017): Additive manufacturing assisted conformal cooling channels in mold manufacturing processes. *Advances in Mechanical Engineering*, vol. 9, no. 5, pp. 1-14.

Shinde, M. S.; Ashtankar, K. M. (2017): Cycle time reduction in injection molding by using milled groove conformal cooling. *Computers, Materials & Continua*, vol. 53, no. 3, pp. 223-234.

Wang, Y. Yu, K. M.; Wang, C. C. L. (2015): Spiral and conformal cooling in plastic injection molding. *Journal Computer Aided Design*, vol. 63, pp. 1-11.

Wang, Y.; Yu, K. M.; Wang, C. C. L.; Zhang, Y. (2011): Automatic design of conformal cooling circuits for rapid tooling. *Journal Computer Aided Design*, vol. 43, no. 8, pp. 1001-1010.

Wei, X.; Chen, W.; Chen, B. (2016): B-spline wavelet on interval finite element method for static and vibration analysis of stiffened flexible thin plate. *Computers, Materials & Continua*, vol. 52, no. 1, pp. 53-71.